

Electronic Supplementary Information for paper titled “*Stimuli-responsive granular crystals assembled by dipolar and multipolar interactions*”.

Section S1. Electric field created by an infinite line of opposite charges. As shown in the main text, electric field generated by a charge placed on the midplane between two infinite parallel conductive plates is equal to the electric field generated by an infinite line of charges (refer to main-text derivation of eq. 3). We represent this infinite line of point charges by periodic charge density $\lambda(z)$ with a period $2d$ (as can be seen from main-text **Fig. 3b**), which can be written as:

$$\lambda(\hat{z}) = \frac{q_1}{d} (\delta(\hat{z}) - \delta(\hat{z} - d) + \delta(\hat{z} - 2d)), \quad \hat{z} \in [0, 2d] \quad (1)$$
$$\lambda(\hat{z} + 2dn) = \lambda(\hat{z}), \quad n \in \mathbb{Z}$$

, where δ is the Dirac delta function. This function can be expressed in the form of Fourier Series:

$$\lambda(z) = 2 \frac{q_1}{d} \sum_{k=0}^{\infty} \cos\left((2k+1) \frac{\pi}{d} z\right) \quad (2)$$

With this charge density function, the electric field created by an infinite series of charges can be represented as:

$$E_x(x) = \frac{1}{4\pi\epsilon_0} \int_{-\infty}^{\infty} \frac{\lambda(z) x}{(x^2 + z^2)^{\frac{3}{2}}} dz$$
$$= \frac{2}{4\pi\epsilon_0} \frac{q_1}{d} \sum_{k=0}^{\infty} \int_{-\infty}^{\infty} \frac{x \cos\left((2k+1) \frac{\pi}{d} z\right)}{(x^2 + z^2)^{\frac{3}{2}}} dz \quad (3)$$

Evaluation of the integral in the infinite sum on the right-hand side of (3) gives:

$$\int_{-\infty}^{\infty} \frac{x \cos(mz)}{(x^2 + z^2)^{\frac{3}{2}}} dz = 2 m K_1(mx) \quad (4)$$

, where K_1 is a modified Bessel function of the second kind, and $m = (2k + 1) \frac{\pi}{d}$. Thus, the electric field in (3) can be written as:

$$E_x(x) = \frac{q_1}{\pi \epsilon_0 d} \sum_{k=0}^{\infty} \left((2k + 1) \frac{\pi}{d} \right) K_1 \left((2k + 1) \frac{\pi}{d} x \right) \quad (5)$$

or, as a function of the dimensionless variable $r = x/d$:

$$E_x(r) = \frac{q_1}{\pi \epsilon_0 d^2} \sum_{k=0}^{\infty} ((2k + 1)\pi) K_1((2k + 1)\pi r). \quad (6)$$

As shown by Yang and Chu (*J. Inequalities Appl.* 2017, **41**, 2017), K_1 can be approximated by:

$$K_1(z) \approx \sqrt{\frac{\pi}{2}} \frac{e^{-z}}{\sqrt{z}} \left(1 + O\left(\frac{1}{z}\right) \right); z \rightarrow \infty. \quad (7)$$

Using this approximation and leaving only the first term in the sum from equation (6), we obtain the following expression for $r > 1$:

$$E_x(r) \approx \frac{q_1}{\pi \epsilon_0 d^2} \frac{\pi}{\sqrt{2}} \frac{e^{-\pi r}}{\sqrt{r}} \quad (8)$$

Section S2. Additional MD simulations of particles in a finite box. We performed another set of MD simulations (hereafter S^{box}) with the aim to capture the effects of physical walls present in the experimental system. The number of particles was $n = 300$ of each type, boundaries represented a square box with side $L = 150$ mm, and agitation pattern was given by the

Weierstrass function. Collisions of particles with the walls and between each other were treated as perfectly elastic (modeled by WCA potential, as in main-text MD simulations with periodic boundaries), and electrostatic interactions were either F_{1p} (main-text eq. 1) or F_{2p} (main-text eq. 7). We assumed that particles have only static and sliding friction, both with a coefficient $\eta = 0.05$, and ignored any effects caused by rolling of the beads. Nylon beads were represented by positively-charging particles having mass of $m_{pos} = 0.0198$ g, whereas particles representing PTFE were charging negatively and had mass $m_{neg} = 0.037$ g. All particles had zero initial charges but charged by $+0.0125$ nC (-0.0125 nC) upon each collision, until reaching the maximum allowed charge of $+0.75$ nC (-0.75 nC) in the case of Nylon (PTFE). Charge of Nylon particles was not only increasing with each collision, but also decayed with first-order kinetics $\frac{dQ}{dt} = -kQ$ with rate constant $k = 0.003$ s $^{-1}$. With this dynamics, average charges at the end of the simulations were remarkably close to the ones measured at the end of the corresponding experiments, as summarized in **Table S2**.

Figure S1 illustrates the results of these simulations for the one and two plates. As in the experiments, crystals grow bigger when the particles interact via F_{2p} , rather than F_{1p} forces (**Fig. S1a** vs. **S1b**), and the proportion of the particles within the domains of square packing is higher ($\sim 45\%$ for F_{1p} and $\sim 62\%$ for F_{2p}). In all of the S^{box} simulations, crystals are larger than in main-text MD simulations with periodic boundary conditions because of two possible reasons: (i) crystals are sometimes hit by the walls of the box, which promotes their reconfiguration and escaping local energy minima, and (ii) beads are more mobile when not charged and incorporated into crystals, which leads to them having higher effective temperature in the beginning of the simulations. Crystals have a tendency to migrate to one corner in S^{box} more than in the

experiments; this can be attributed to the fact that there is only sliding friction in S^{box} , which leads to beads moving mostly in the direction of box agitation. In contrast, in the experiments friction is much more complex, and beads move in other directions due to additional regimes of motion such as rolling, rubbing against each other, etc.

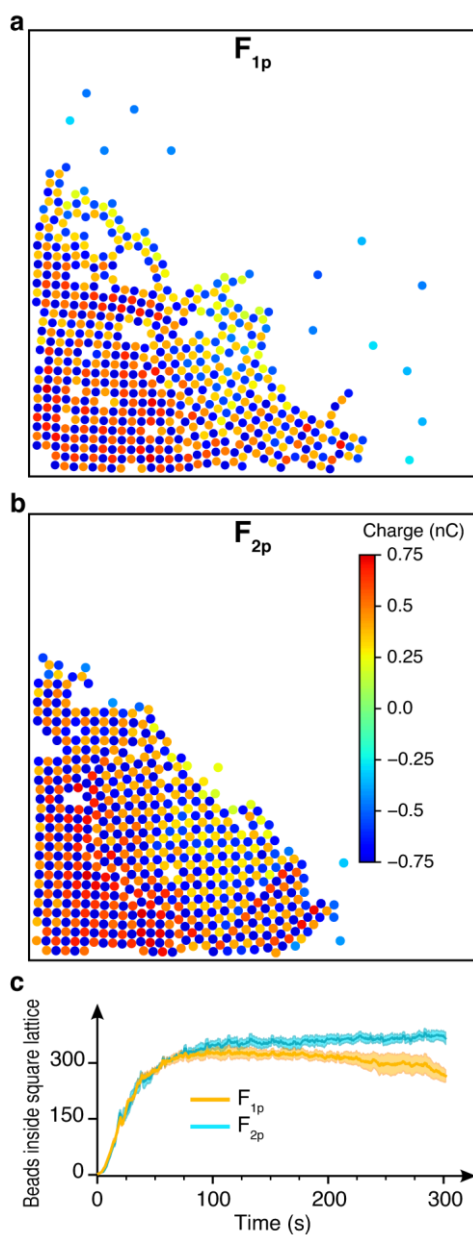


Figure S1. MD simulations of the formation of non-electroneutral, square-lattice crystals in experimental box, S^{box} . (a,b) Snapshots from simulations of crystals self-assembled from 300

negatively-charging and 300 positively-charging particles agitated for 5 minutes. Simulations using interaction forces F_{1p} (**a**) and F_{2p} (**b**) represent experiments with one and two conductive plates, respectively. Colors on the images indicate charges of the particles (quantified in the legend). (**c**) Average number of beads inside the square lattice over the time of the simulations, each curve represents the average of $n = 3$ simulations and shaded regions indicate one standard deviation.

Section S3. Analytical balance measurement of interaction between a charged bead and its

image charge. Before the measurements, agitation was performed for 5 minutes in $L = 100$ mm

box with $n = 150$ beads of each of two types: charging positively (Nylon, Acryl) and negatively (PTFE). The measurement setup is illustrated in **Fig. S2** and was used as described below.

Immediately after agitation, one of the beads from inside a crystal was picked up by antistatic tweezers and placed on a flat end of a wooden post (about 1 mm in diameter) covered with a very thin layer of cyanoacrylate glue. The post with the bead was transferred to an analytical balance

(equipped with a post holder) and a grounded conductive plate was brought to a distance within

$50 \mu\text{m}$ from the bead using a linear stage. The data from analytical balance was recorded by a

computer (PC) connected via USB. This procedure, when performed in a timely manner, allowed

us to start recording in about 1 minute after the end of agitation. It should be noted that the

described manipulations inevitably cause some leakage of charge away from the beads, especially

the ones made out of Nylon (which is expected since conductivity of Nylon is $\sigma = 10^{-12}$ S/m, orders

of magnitude higher than that of PTFE, $\sigma = 10^{-24}$ S/m, or Acryl, 10^{-19} S/m), so the measured values

do not reflect the total charge accumulated on the beads or exact discharge profile of beads in the

experimental box. Nevertheless, the results obtained from these measurements provide us with a

reasonable basis to conclude that discharge of Nylon beads is a primary reason for the observed non-electroneutrality of the crystals.

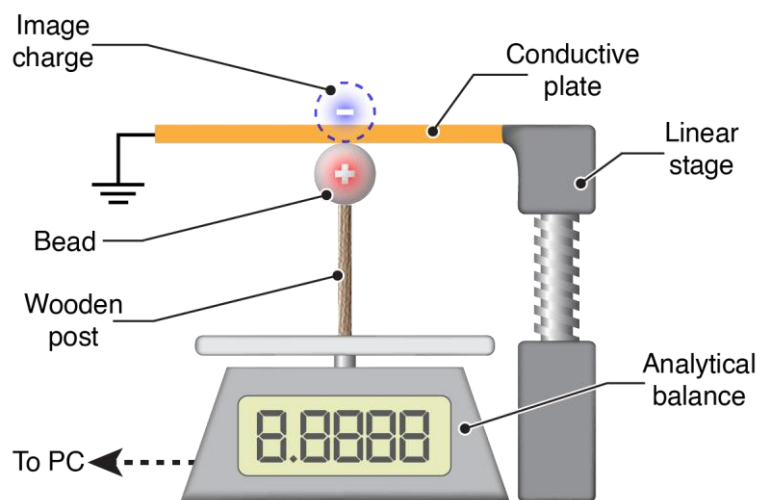


Figure S2. Analytical balance setup for quantifying interaction between a bead and its image charge.

Section S4. Additional force calculations.

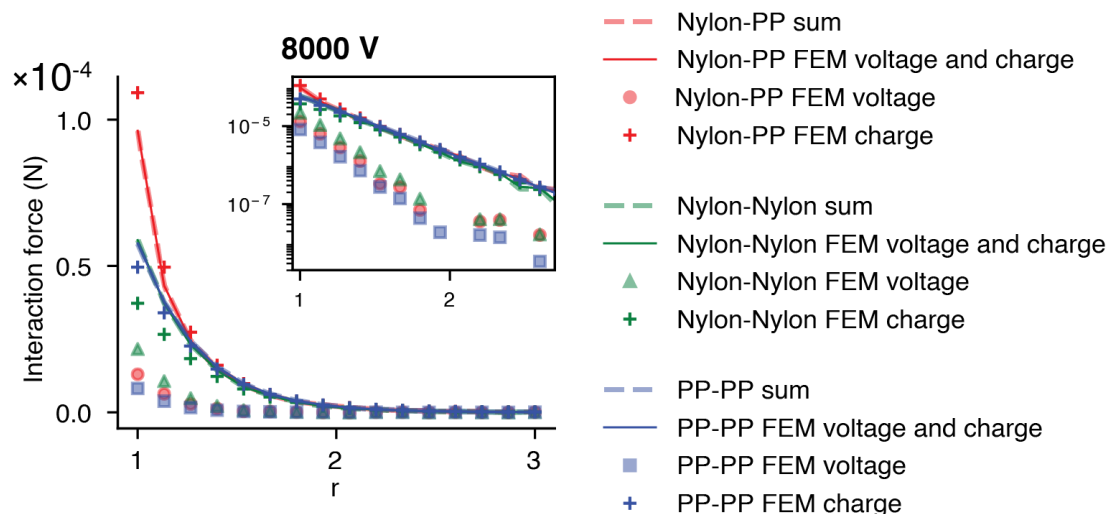


Figure S3. Additivity of interactions due to beads' charge and voltage-induced dipoles.

Plotted are attraction forces, obtained by FEM calculations, between a pair of Nylon and polypropylene (PP) beads having, respectively, $+0.45$ nC and -0.45 nC charges and placed between two conductive plates. “FEM charge” forces (“+” markers) are for charged beads without voltage bias between the plates; “FEM voltage” forces (square markers) are for beads without charge but with 8 kV bias applied between the plates; “FEM voltage and charge” forces (solid lines) are for the case when beads were charged and 8 kV bias was applied; “sum” curves (dashed lines) are obtained by summing up “FEM charge” and “FEM voltage” curves. Matching of “sum” with “FEM voltage and charge” curves demonstrates the additivity of interactions.

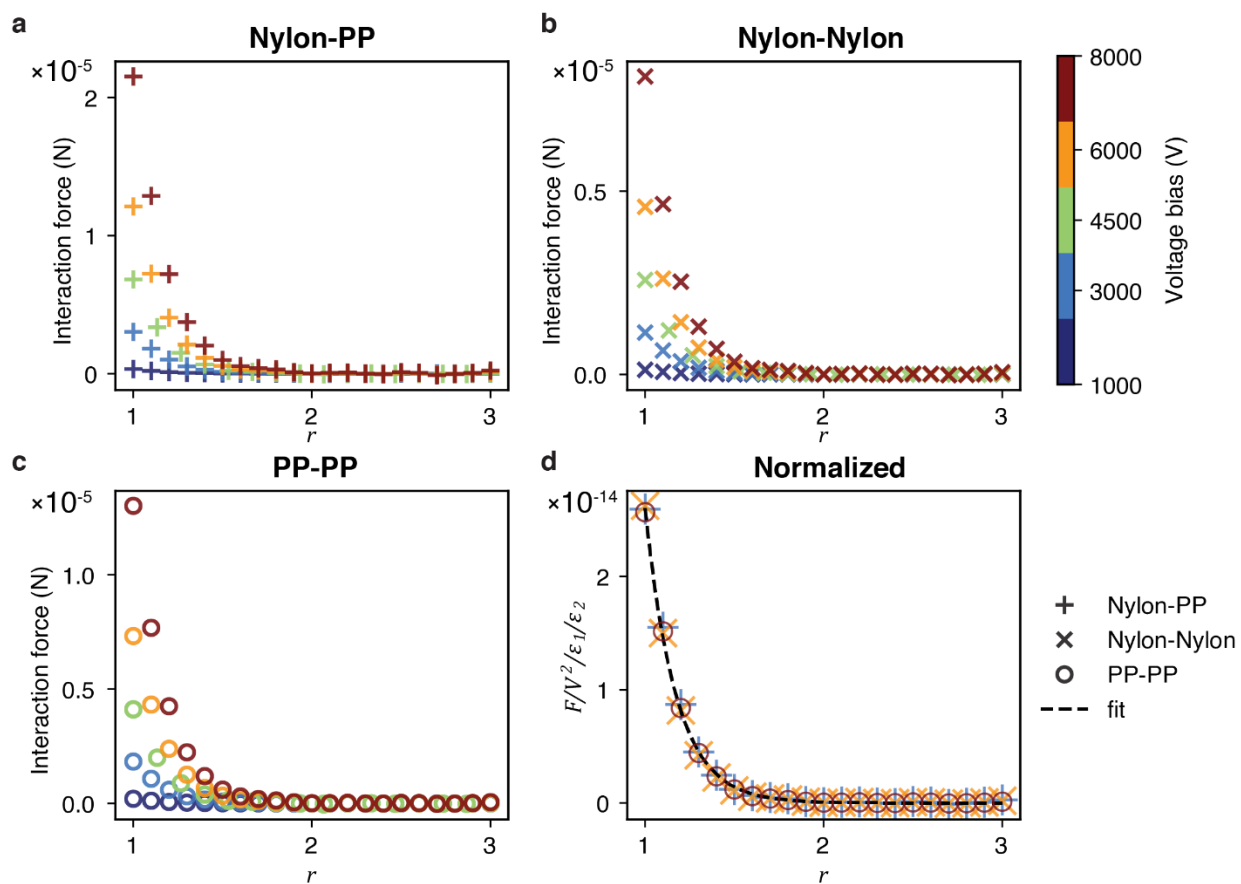


Figure S4. Voltage-induced interactions quantified by FEM calculations. Panels (a-c) plot magnitudes of interactions between non-charged beads separated by center-to-center distance r and placed between two conductive plates with voltage bias applied: Nylon-PP (a), Nylon-Nylon (b), and PP-PP (c). Magnitude of voltage bias are indicated by the colorbar in the upper right. Panel (d) shows that interactions with different voltages can be represented by one exponential fit – in particular, normalization of forces by dielectric constants (ϵ_1 and ϵ_2) of interacting beads and squared magnitude of voltage bias applied between the plates (V^2) yields matching curves for different beads and voltage biases. The resulting exponential fit is shown in dashed line.

Arrangement	Fitting function	Materials of interacting beads	a	b
1 plate	ax^{-b}	Nylon-PTFE	9.78×10^{-14}	3.74
		Nylon-Nylon	1.06×10^{-12}	3.15
		PTFE-PTFE	1.72×10^{-12}	3.24
2 plates	ae^{-bx}	Nylon-PTFE	3.65×10^{-3}	1.12×10^3
		Nylon-Nylon	1.13×10^{-3}	1.03×10^3
		PTFE-PTFE	3.19×10^{-3}	1.04×10^3

Table S1. Fitting parameters obtained from FEM simulations.

	Experiments		Simulations S^{box}	
	Nylon, nC	PTFE, nC	Positive particles, nC	Negative particles, nC
1 plate	$+0.44 \pm 0.05$	-0.67 ± 0.01	$+0.44 \pm 0.03$	-0.67 ± 0.02
2 plates	$+0.42 \pm 0.06$	-0.64 ± 0.02	$+0.47 \pm 0.03$	-0.70 ± 0.02

Table S2. Bead charges measured after crystallization experiments and used in simulations S^{box} . For each type, $n = 15$ beads were measured after the experiment, and data for all particles ($n = 300$ of each) was collected from simulations. “ \pm ” values give one standard deviation.

Section S5. Lattice classification using different definitions of bond-order parameters.

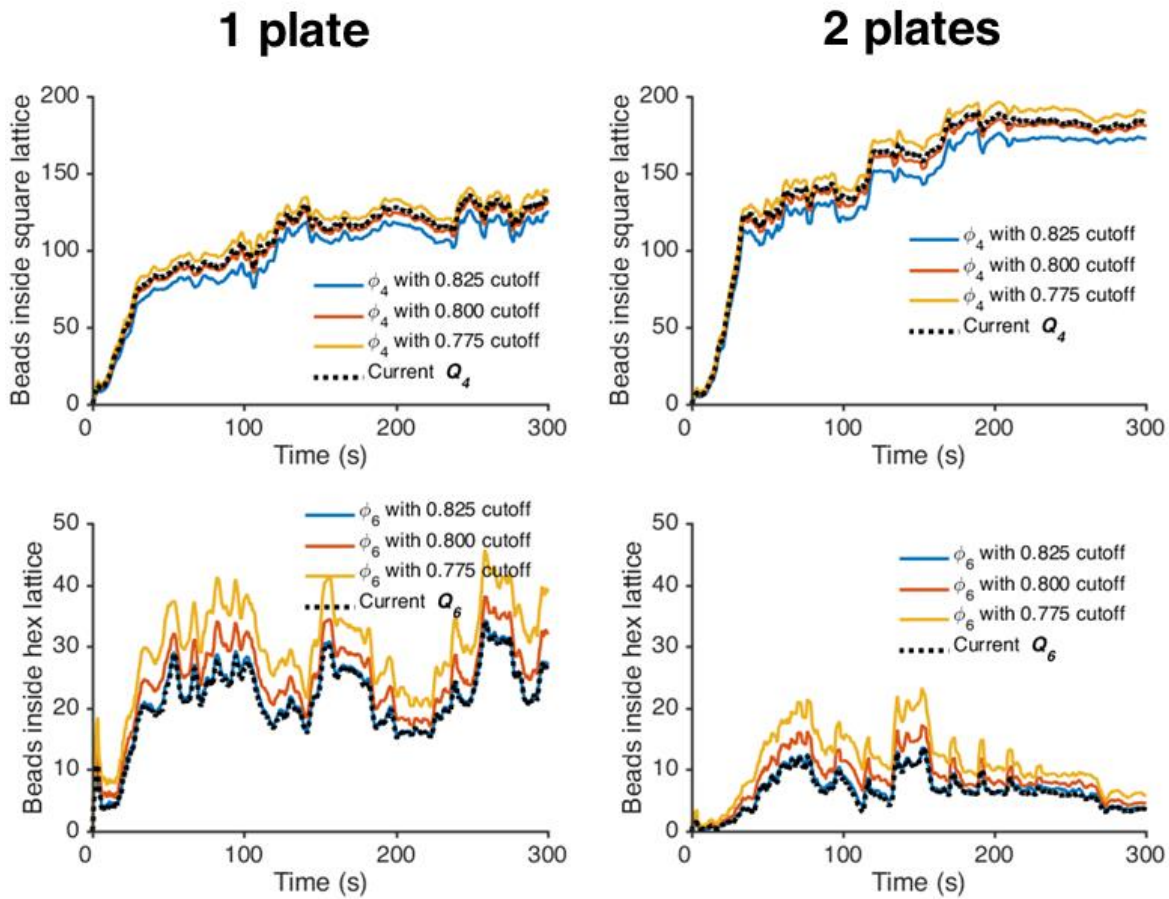


Fig. S5. Comparison of detecting beads inside square vs. hexagonal lattices using different bond-order parameter definitions. Left plots use data from the experiment shown in main-text **Fig. 2a** with one conductive plate, plots on the right – in the main-text **Fig. 2b** with two conductive plates. Top plots show in black dotted lines Q_4 that correspond to curves in main-text **Fig. 1c**; similarly, bottom plots show Q_6 from main-text **Fig. 1d**. Other curves trace local bond-orientational order parameters ϕ_4 and ϕ_6 defined as $\phi_s = \langle \frac{1}{N_b} \sum_{n=1}^{N_b} e^{si\theta_n} \rangle$ where N_b is the number of "bonds" with neighboring particles, s is the symmetry number (4 for square lattice, 6 for hexagonal), and θ_n is the angle to the n -th neighbor.

Movie captions:

Supplementary Video S1. Self-assembly of non-electroneutral crystals agitated on one conductive plate. Overlaid is color shading that indicates structural invariant values Q_4 and Q_6 of beads, which depend on whether a bead is inside the square (blue, Q_4) or hexagonal (red, Q_6) lattice; colorbars with corresponding colors show Q_4 and Q_6 values. Histogram on the right shows the number of beads having certain structural invariant value.

Supplementary Video S2. Self-assembly of non-electroneutral crystals between two conductive plates. Overlaid is color shading that indicates structural invariant values Q_4 and Q_6 of beads, which depend on whether a bead is inside the square (blue, Q_4) or hexagonal (red, Q_6) lattice; colorbars with corresponding colors show Q_4 and Q_6 values. Histogram on the right shows the number of beads having certain structural invariant value.

Supplementary Video S3. Reversible transformation of crystals into porous or filamentous structures upon application of, respectively, 4.5 kV and 8 kV votalge bias.